



**HAL**  
open science

## Modifying internal organization and surface morphology of siRNA lipoplexes by sodium alginate addition for efficient siRNA delivery

Danielle Campiol Arruda, Ismael José Gonzalez, Stéphanie Finet, Luis Córdova, Valérie Trichet, Gracielle Ferreira Andrade, Céline Hoffmann, Pascal Bigey, Waldemar Augusto de Almeida Macedo, Armando da Silva Cunha Jr, et al.

### ► To cite this version:

Danielle Campiol Arruda, Ismael José Gonzalez, Stéphanie Finet, Luis Córdova, Valérie Trichet, et al.. Modifying internal organization and surface morphology of siRNA lipoplexes by sodium alginate addition for efficient siRNA delivery. *Journal of Colloid and Interface Science*, 2019, 540, pp.342-353. 10.1016/j.jcis.2019.01.043 . hal-02360726

**HAL Id: hal-02360726**

**<https://hal.science/hal-02360726>**

Submitted on 15 Nov 2019

**HAL** is a multi-disciplinary open access archive for the deposit and dissemination of scientific research documents, whether they are published or not. The documents may come from teaching and research institutions in France or abroad, or from public or private research centers.

L'archive ouverte pluridisciplinaire **HAL**, est destinée au dépôt et à la diffusion de documents scientifiques de niveau recherche, publiés ou non, émanant des établissements d'enseignement et de recherche français ou étrangers, des laboratoires publics ou privés.

## **MODIFYING INTERNAL ORGANIZATION AND SURFACE MORPHOLOGY OF siRNA LIPOPLEXES BY SODIUM ALGINATE ADDITION FOR EFFICIENT siRNA DELIVERY**

Danielle Campiol Arruda<sup>1,2,3,4,5</sup>, Ismael José Gonzalez<sup>6</sup>, Stéphanie Finet<sup>7,8,9,10</sup>, Luis Cordova<sup>11,12,13</sup>, Valérie Trichet<sup>12,13</sup>, Gracielle Ferreira Andrade<sup>1</sup>, Céline Hoffmann<sup>2,3,4,5</sup>, Pascal Bigey<sup>2,3,4,5</sup>, Waldemar Augusto de Almeida Macedo<sup>6</sup>, Armando Da Silva Cunha Jr<sup>1</sup>, Angelo Malachias de Souza<sup>14</sup>, Virginie Escriou<sup>2,3,4,5\*</sup>

<sup>1</sup> Faculdade de Farmácia, Universidade Federal de Minas Gerais, 31270-901, Belo Horizonte, MG, Brasil

<sup>2</sup> CNRS, Unité de Technologies Chimiques et Biologiques pour la Santé (UTCBS) UMR 8258, F-75006 Paris, France

<sup>3</sup> INSERM, UTCBS U 1022, F-75006 Paris, France

<sup>4</sup> Université Paris Descartes, Sorbonne-Paris-Cité University, UTCBS, F-75006 Paris, France

<sup>5</sup> Chimie ParisTech, PSL Research University, UTCBS, F-75005 Paris, France

<sup>6</sup> Centro de Desenvolvimento da Tecnologia Nuclear, CDTN, 31270-091, Belo Horizonte, MG, Brasil

<sup>7</sup> CNRS, Institut de minéralogie, de physique des matériaux et de cosmochimie (IMPMC) UMR 7590, F-75005, Paris, France

<sup>8</sup> Sorbonne Université, IMPMC, F-75005 Paris, France

<sup>9</sup> IRD, IMPMC, F-75005 Paris, France

<sup>10</sup> MNHN, IMPMC, F-75005 Paris, France

<sup>11</sup> Department of Oral and Maxillofacial Surgery, Faculty of Dentistry, University of Chile, 8380000, Santiago, Chile.

<sup>12</sup> INSERM, UMR 957, Equipe Labellisée LIGUE 2012, F-44035 Nantes, France

<sup>13</sup> Université de Nantes, Nantes Atlantique Universités, Laboratoire de Physiopathologie de la Résorption Osseuse et Thérapie des Tumeurs Osseuses Primitives, Faculté de Médecine, F-44035 Nantes, France

<sup>14</sup> Departamento de Física, Universidade Federal de Minas Gerais, 31270-901, Belo Horizonte, MG, Brasil

\* Corresponding author: Dr. Virginie ESCRIOU

UTCBS, CNRS UMR 8258, Faculté de Pharmacie, 4 avenue de l'Observatoire, 75270 Paris cedex 06, France Tel: 33 1 53 73 95 75 Fax: 33 1 70 64 94 52 virginie.escriou@parisdescartes.fr

**Keywords:** RNA interference; cationic lipid; nanoparticle; delivery system; structure; anionic polymer

**Declarations of interest:** none

## ABSTRACT

Vectorized small interfering RNAs (siRNAs) are widely used to induce specific mRNA degradation in the intracellular compartment of eukaryotic cells. Recently, we developed efficient cationic lipid-based siRNA vectors (siRNA lipoplexes or siLex) containing sodium alginate (Nalg-siLex) with superior efficiency and stability properties than siLex. In this study, we assessed the physicochemical and some biological properties of Nalg-siLex compared to siLex. While no significant differences in size,  $\zeta$  potential and siRNA compaction were detected, the addition of sodium alginate modified the particle morphology, producing smoother and heterogeneous particles characterized by Transmission Electron Microscopy. We also noted that Nalg-siLex have surface differences observed by X-ray Photoelectron Spectroscopy. These differences could arise from an internal reorganization of components induced by the addition of sodium alginate, that is indicated by Small-Angle X-ray Scattering results. Moreover, Nalg-siLex did not trigger significant hepatotoxicity nor inflammatory cytokine secretion compared to siLex. Taken together these results suggest that sodium alginate played a key role by structuring and reinforcing siRNA lipoplexes, leading to more stable and efficient delivery vector.

## 1. Introduction

RNA interference (RNAi) is a natural phenomenon mediated by small double-stranded RNA oligonucleotides, called small interfering RNAs (siRNAs) [1]. siRNAs specifically silence target genes by binding to a multi-protein nuclease complex called RNA-induced silencing complex (RISC), recruiting their complementary mRNA and guiding the nuclease for the sequence-specific cleavage of the mRNA. siRNAs have also been reported to hybridize to their mRNA target with high degree of specificity. Therefore, the opportunity for mediating highly specific gene silencing of any target gene of a eukaryotic organism's genome has opened the way for a drug development field which is now regarded not only as research tool but also as innovative therapeutic applications [2-3]. The most common method used to harness the RNAi pathway for targeted gene silencing is to deliver synthetic versions of 21-22nt siRNAs into cells. However, in order to induce the degradation of their complementary mRNA, RNAi-based therapies need to be transported to the cytoplasm of target cells, where the RNAi machinery is located. Unmodified RNA duplex oligonucleotides are also known to be poorly resistant to nuclease-containing environments. Their large size and weight (around 13 kDa) and their global negative charge (due to around 40 phosphate groups) preclude their entry into cells. Consequently, a growing number of delivery vehicles have been proposed to mediate siRNA delivery into cells [4]. Among them, delivery systems based on lipids are the most widely used materials [5]. Cationic lipids can condense nucleic acids into a cationic particle, called lipoplex, when the two components are mixed together. Once encapsulated into lipoplexes, siRNAs are protected from enzymatic degradation and delivered into cells by interaction of the particle with the negatively charged cell membrane. Unlike more recently described types of lipid-based nanoparticles (SNALP, SPLP, LDP, NLP, reviewed in [6]), lipoplexes are not ordered nucleic acid phase surrounded by an external lipid bilayer, rather they are partially condensed nucleic acid complexes with an ordered substructure and irregular morphology [6]. Also, they are simple nucleic acid delivery systems, because of the small number of their components, easy and quick to prepare in one step in an aqueous buffer, and not requiring a long-lasting or sophisticated step such as dialysis or microfluidics. We have recently described the enhanced gene silencing efficacy of a new type of siRNA delivery system based on cationic lipid and anionic polymer [7] (Fig. 1). This innovative vector (patented in [8]) is obtained by self-assembly of a cationic liposome and a mixture of siRNA and anionic polymer. In particular, we observed that the anionic polymer sodium alginate contributed to increased stability of the delivery system upon incubation in biological medium, as well as to prolonged integrity of siRNA once complexed in the particle [9]. Other groups have also included alginate in polyplexes (nucleic acid / cationic polymer complexes), triggering enhanced transfection efficiency and maintenance of low cytotoxicity when compared to nanoparticles formed without its addition [10-11]. It was also suggested that higher transfection efficiency of chitosan / alginate / plasmid DNA

polyplexes was related to the reduced interaction between the polycationic polymer and plasmid DNA, triggered by alginate which facilitates plasmid DNA release in cultured cells [12].

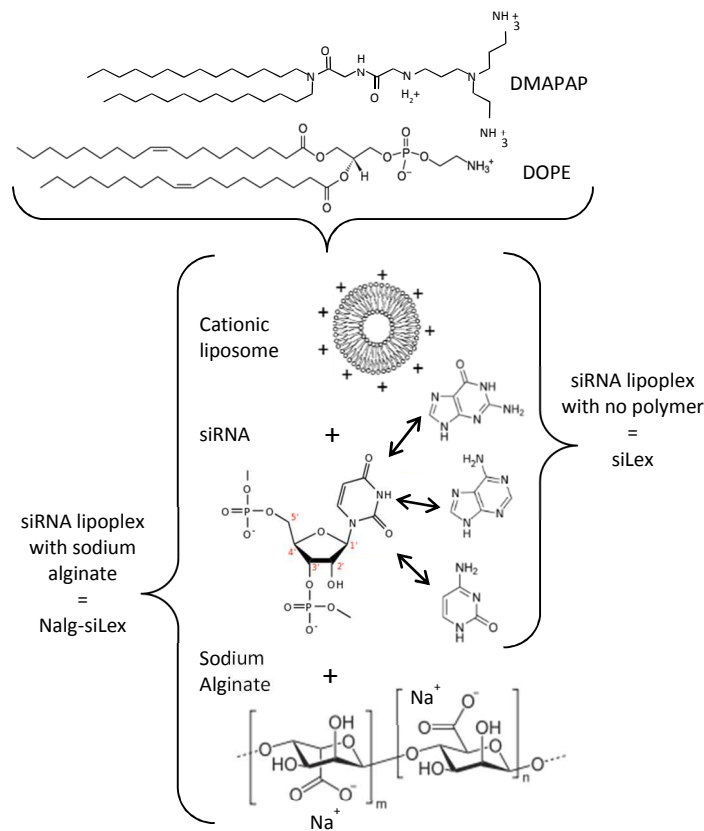


**Fig. 1.** Components and particles used in this work. Cationic liposomes are composed of an equimolar mixture of cationic lipid DMAPAP and zwitterionic lipid DOPE. siRNA lipoplexes obtained by auto-assembly of siRNA and DMAPAP / DOPE liposomes are called siLex, those containing also sodium alginate are called Nalg-siLex.

Unlike these groups, we have designed sodium alginate-supplemented siRNA lipoplexes (or Nalg-siLex) to solidify the obtained particles rather than to enhance siRNA release. Indeed, we hypothesized that alginate, bearing negative charges, would be capable to mix with siRNA and take part in the auto-assembly of particles by forming electrostatic interactions with the positive charges of cationic lipid head groups. We have shown, using an electrophoretic technique, that alginate is associated with the particle (additional data of [7]). The obtained particles were more efficient for gene silencing than lipoplexes prepared with no anionic polymer (siLex) [7] but so far the effect of adding anionic polymer on the particle structure remains under investigation.

Lipoplexes formation mechanism and the steps leading to their formation have been most intensively studied, particularly for lipoplexes with plasmid DNA (pDNA) (reviewed in [13]). Lipoplex self-assembly is driven by electrostatic attraction between the oppositely charged nucleic acids and lipids. The equilibrium structures resulting from these interactions are controlled by the lipid type (composition of mixtures), as well as by the +/- charge ratio, defined as the ratio between the

positive charges brought by the cationic lipid and the negative charges of DNA. Qualitatively, it is expected that siRNA lipoplexes would be similar to pDNA lipoplexes, since siRNA and pDNA are both double-stranded (ds) nucleic acids. They have anionic phosphodiester backbones with the same negative charge to nucleotide ratio and both can interact electrostatically with cationic agents. However, siRNA is hundred times smaller than pDNA, which may influence the formation of the particles. pDNA has a molecular topography which allows its condensation into small, nanometric particles when complexed with a cationic agent, while 21 bp siRNAs behave as rigid rods not likely to further condense. In contrast to pDNA, siRNA may then retain its initial structure after interaction with the positively charged lipid. Only a few studies aimed to link the structure of siRNA delivery vectors to their efficiency have been performed and reported [14-17]. The aim of this work is to extensively study the structural and physico-chemical characteristics of siRNA lipoplexes prepared with sodium alginate (Nalg-siLex) as compared to siRNA lipoplexes without alginate (siLex), in order to characterize the effects of addition of alginate. It is valuable to study in parallel two types of particles having different gene silencing efficiency, making it possible to obtain information on the structure-function relation of the particles, increasing knowledge of this kind of delivery systems and even opening a path to improve the existing system.

We found significant differences between Nalg-siLex and siLex, in terms of morphology, surface properties and structure.

## 2. Materials and methods

### 2.1. Materials

siRNA (unmodified) specific to luciferase (5' CUU ACG CUG AGU ACU UCG AdTdT 3') or non-silencing siRNA used as negative control (5' UUC UCC GAA CGU GUC ACG UdTdT 3') were obtained from Eurogentec. Sodium alginate was purchased from Sigma-Aldrich (reference 180947). DOPE (1,2-dioleoyl-sn-glycero-3-phosphoethanolamine) was from Avanti Polar Lipids.

### 2.2. Preparation of cationic liposome and siRNA lipoplexes

Cationic liposomes containing DMAPAP cationic lipid 2-{3-[Bis-(3-amino-propyl)-amino]-propylamino}-N-ditetradecylcarbamoyl methyl-acetamide (synthesized as described in [18]) and DOPE in equimolar amounts were prepared as described in [7]. siLex were prepared by mixing an equal volume of the siRNA solution diluted in 150 mM NaCl to the cationic liposome dispersion prepared also in 150 mM NaCl and rapidly mixed by vortexing. For Nalg-siLex, siRNA and sodium alginate were mixed in 150 mM NaCl (ratio 1/1, w/w) before adding to cationic liposomes. Lipoplexes were allowed to form at least for 30 min at room temperature before use. The +/- charge ratio (+/- R) was calculated using the molar ratio of positive charges (3 positive charges per molecule of DMAPAP) and the molar ratio of negative charges (from siRNA and sodium alginate, siRNA 3.03 and sodium alginate 5.05 nmoles of negative charges/ $\mu$ g, respectively). As a result, for particles prepared at the same +/- R and at the same siRNA concentration, Nalg-siLex contain 2.7 times more lipids than siLex.

### 2.3. Size and $\zeta$ potential measurements

Size and  $\zeta$  potential measurements were performed on a MALVERN Zetasizer Nanoseries Nano ZS. siLex and Nalg-siLex were prepared in 100  $\mu$ l of NaCl 150 mM with a final concentration of siRNA of 334 nM. For  $\zeta$  potential measurements, lipoplexes (siRNA 33.4 nM) were prepared in 15 mM NaCl.

### 2.4. siRNA complexation assay

siRNA complexation was evaluated by measuring the accessibility of the fluorescent dye RiboGreen to siRNA with a microplate reader (Wallac Victor<sup>2</sup>, excitation 485 nm, emission 525 nm). Hundred  $\mu$ l of a RiboGreen dilution (1/200) were added to 100  $\mu$ l of lipoplexes (siRNA 17 nM). Blanks containing no lipid or no siRNA were also prepared. Results are presented as percentage of samples without cationic liposome.

### 2.5. Transmission Electron Microscopy (TEM)

A drop (20  $\mu$ l) of lipoplexes dispersion (siRNA concentration 400 nM) was first applied onto a Formvar/carbon copper grid 200 mesh from Agar Scientific pre-treated with Bacitracine 0.1 % (w/v),

allowed to adsorb for 2 min, and blotted with filter paper. A drop of 4 % (w/v) aqueous uranyl acetate stain was applied to the sample grid, allowed to stain for 2 min, blotted with filter paper and air drying for 4 min. Analyses were performed on a microscope JEOL, JEM 100S.

### *2.6. X-ray Photoelectron Spectroscopy (XPS)*

XPS analysis was performed on a Specs surface analysis system equipped with a Phoibos 150 electron analyzer using a monochromatized Al K $\alpha$  radiation (1486.6 eV) at a power of 350 W. An electron flood gun operating at 0.1  $\mu$ A was used to compensate the charge effect in the samples and the C 1s signal (284.6 eV) was employed as reference for the calibration of the binding energies (BE) of different elements. CasaXPS software was used to process the analysis data and to estimate the samples surface atomic concentrations. Deconvolution of C 1s and N 1s signal was carried out setting up the FWHM of synthetic bands between 1.7 and 2.2 eV. Lipoplexes were prepared at final siRNA concentration of 5.0  $\mu$ M in 128 or 138 mM NaCl for Nalg-siLex and siLex, respectively. The liposome dispersion used was at 20 mM lipid concentration. The sample preparation for XPS analysis required the fixation of liposome and lipoplexes dispersions on the sample holder slides using graphite adhesive tape and consecutive steps of drop drying in the desiccator until obtaining a thick and stable film over the tape.

### *2.7. Small-angle X-ray scattering (SAXS)*

SAXS measurements were carried out at the SWING beamline of SOLEIL (Gif-sur-Yvette, France), using a fixed energy of 12.4 keV. A PCCD170170 (AVIEX) detector was placed at a 1.5 m distance from the sample, covering a momentum scattering vector (Q) range that spans from 0.3 until 5 nm<sup>-1</sup>. In this setup a resolution of 0.002 nm<sup>-1</sup> is achieved. All datasets shown are obtained after an angular integration of the detector area ("cake", using FIT2D routines). Suspensions of liposomes and siRNA lipoplexes in NaCl 150 mM were inserted manually into a capillary. In this work all measured scattering patterns are angularly isotropic. siLex and Nalg-siLex were prepared in 100  $\mu$ l of NaCl 150 mM with a final concentration of siRNA of 19  $\mu$ M or 38  $\mu$ M. Cationic liposome suspension at 20 mM was diluted with NaCl 150 mM solution to obtain different lipid concentrations of 10.0, 5.0, 1.0 and 0.5 mM.

### *2.8. Gene silencing and cellular viability on cultured cells*

B16-Luc were obtained by stable incorporation into the genome of B16-F0 cells the firefly luciferase gene and grown as described [19]. B16-Luc cells were transfected as described [7] with lipoplexes prepared at increasing siRNA concentrations (see legend of Fig. 6) for 24 h in 24-well plates. 48 h later, the transfected cells were washed twice with PBS and lysed, and luciferase and total protein

were assayed as in [7]. The results, calculated in cps (count per second), were normalized to the total protein concentration of each sample and the gene silencing efficiency was expressed as the luciferase activity inhibition percentage relative to the luciferase activity of non-transfected control cells. Cellular viability was assayed on transfected B16 cells using the MTT test as described [7].

### *2.9. Innate immune stimulation and hepatotoxicity*

*In vivo* experiments were conducted according to the local ethical committee recommendations for animal experimentation (registered number CEEA34.AS.038.11). Six-week-old female C57Bl/6 mice (Janvier) were anesthetized by *i.p.* injection of a mix of ketamine (100 mg/kg) and xylazine (10 mg/kg). A 200  $\mu$ l volume of Control-siRNA lipoplexes (+/- R 8, 1 mg siRNA/kg) was injected into the retro-orbital sinus of the mouse. Blood was collected 2 h, 6 h or 24 h after injection. Cytokines levels were assayed using ELISA kits (DuoSet ELISA for mouse TNF- $\alpha$ , IL-6 and IFN- $\gamma$  from R&D Systems, Verikine mouse INF- $\alpha$  and INF- $\beta$  ELISA kits from PBL InterferonSource). ALT (Alanine Aminotransferase) was assayed using ALT activity assay kit from Biovision.

### *2.10. Statistical analysis*

All experimentation results were analyzed with the unpaired non parametric Mann-Whitney test using two-tailed P-values. Results with  $p < 0.05$  were considered significant.

### 3. Results

#### 3.1. Size, $\zeta$ potential and siRNA complexation

Size and colloidal stability of siRNA lipoplexes are highly dependent on the +/- charge ratio (+/- R) at which they are prepared. Indeed, a significant increase in the size and variance of size can be observed when their  $\zeta$  potential approaches zero. At this point, the net charge on the surface of particles is neutral or “isoelectric”, which relieves the repulsive electrostatic force which otherwise prevents the aggregation of charged particles. We first compared the size and the  $\zeta$  potential of siLex and Nalg-siLex prepared at +/- R of 8. For Nalg-siLex, the presence of negative charges introduced by the addition of the polymer (5.05 nmoles of negative charge per  $\mu\text{g}$  of sodium alginate) was taken into account when calculating the +/- R and resulted in the addition of 2.7 times more lipids in Nalg-siLex than in siLex (see Materials and Methods and first paragraph of Discussion).

**Table 1**

Particles size, polydispersion index (pdi) and  $\zeta$  potential measurements at +/- R of 8. Values are given as mean +/- standard variation.

Sample	Size (nm)	pdi	$\zeta$ potential (mV)
siLex	268 +/- 87 (n=4)	0.747 +/- 0.151 (n=4)	63 +/- 9 (n=6)
Nalg-siLex	182 +/- 9 (n=3)	0.295 +/- 0.049 (n=3)	59 +/- 15 (n=4)

As shown in Table 1, siLex and Nalg-siLex exhibited particle size smaller than 300 nm at +/- R of 8, with clearly higher pdi values for siLex, indicating a much higher polydispersity. Regarding lipoplexes formed by a combination of nucleic acid and cationic lipid, it is known that the size of the obtained particle depends primarily on its +/- charge ratio and not on the size of the incorporated nucleic acid. For example, we and other have shown that for the same +/- charge ratio, siRNA lipoplexes are not smaller than plasmid DNA lipoplexes, even though siRNAs are much smaller than plasmid DNA [7, 20-21]. We also measured  $\zeta$  potential of siLex and Nalg-siLex and observed equivalent and above 50 mV values. Once complexed, nucleic acids are compacted and become unreachable by nucleic acid-binding molecules. In order to monitor the complexation of siRNA upon formation of siRNA lipoplexes, we used the Ribogreen intercalation assay, based on Quant-iT™ RiboGreen® RNA reagent, a dye that becomes intensely fluorescent when bound to RNA. When +/- R increases, Ribogreen fluorescence progressively decreases as a consequence of progressive complexation of siRNA with the cationic lipid.

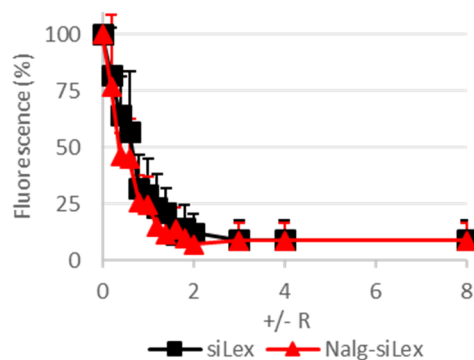


**Fig. 2.** Ribogreen fluorescence of siRNA in the presence of increasing amounts of lipid. Values are given as percentage of the fluorescence assayed with siRNA or siRNA + sodium alginate without addition of cationic liposomes taken as 100%. Mean +/- standard variation, n=3.

As shown in Fig. 2, a significant quenching of the Ribogreen fluorescence was achieved at +/- R of 2, which indicates a high degree of siRNA complexation with cationic liposomes. One also observed that the addition of sodium alginate did not affect siRNA complexation with cationic liposomes. Therefore, it appears that the presence of alginate did not modify the size or  $\zeta$  potential values, but makes it possible to obtain particles whose size was less dispersed. Nalg-siLex has similar characteristics as siLex in terms of degree of siRNA complexation.

### 3.2. Morphology analyses of siLex and Nalg-siLex

Negative staining and TEM were carried out in order to visualize siLex and Nalg-siLex morphology. Images on Fig. 3 show both types of siRNA lipoplexes gave rise to the formation of distinct particles, displaying condensed multilamellar structures, suggesting that the addition of sodium alginate did not prevent the formation of such bilayer structures. However, the addition of sodium alginate modified the global arrangement of these lamellae, since siLex appeared as flower-shaped lamellae whereas Nalg-siLex showed concentric lamellae covering part of the surface of the particle. In addition, Nalg-siLex had a smoother appearance than siLex.

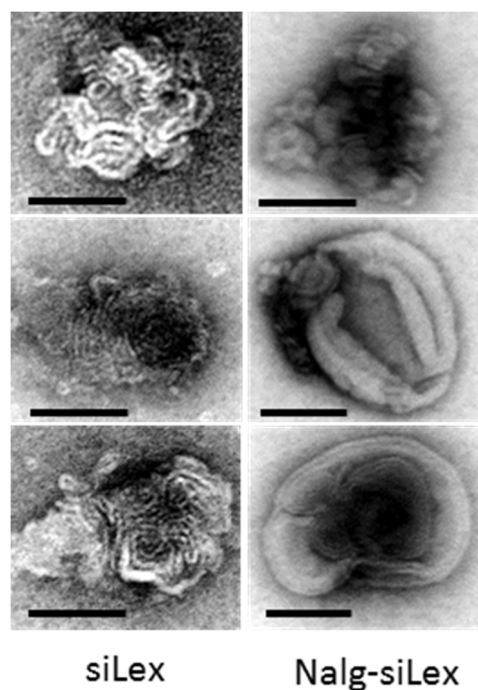


**Fig. 3.** TEM micrographs of siLex and Nalg-siLex (+/- R of 8) after negative staining with uranyl acetate. Each column shows three photos taken for each sample, as indicated. The scale bar is fixed to 100nm.

### 3.3. Surface analyses of siLex and Nalg-siLex - XPS

We further investigate the surface of Nalg-siLex and siLex using X-ray photoelectron spectroscopy (XPS). This technique has already been used to characterize the surface (approximately 5-10 nm penetration depth) chemical composition in different systems, including polymeric microparticles [22] and lipid/polymeric nanoparticles [23-25]. However, to our knowledge, it has never been used to characterize the surface of lipoplexes. Since lipoplexes are particles composed of various components (see Fig. 1), we first assayed separately each constituent molecule, DMAPAP, DOPE, siRNA and alginate. Liposome was also analyzed as a reference for lipid signals and to get an easier data interpretation. The upper part of Table 2 gives the elemental composition of each molecule, including sodium and chloride ions from saline solution or as counter-ion of DMAPAP and alginate. The results obtained for lipids, DMAPAP and DOPE, are very close to the expected values considering their atomic composition (see Fig. S1A for atomic composition). For siRNA and alginate, more complex molecules, the data are globally consistent with their atomic composition as well. We used these values to calculate the expected atomic composition of particles, liposomes and lipoplexes (lower part of Table 2), taking into account the relative proportions of each molecule used to prepare them (see legend of Table 2).

**Table 2**

XPS surface elemental composition of molecules and particles (lipoplexes +/- R of 8).

Sample	Surface composition (At. %) – Measured values					
	O 1s	N 1s	C 1s	Cl 2p	P 2p	Na 1s
DMAPAP	5.5	8.2	79.5	6.8	0	0
DOPE	14.7	2.3	80.2	0	2.8	0
siRNA	22.2	7.6	56.9	9.2	1.7	2.4
Alginate <sup>a</sup>	27.1	0	65.2	4	0	2.9

	Surface composition (At. %) – Measured values					
	O 1s	N 1s	C 1s	Cl 2p	P 2p	Na 1s
Liposome	6.4	6.7	80.6	5.5	0.8	0
siLex	9.2	6.6	73.7	8.0	1.1	1.3
Nalg-siLex	9.1	6.7	73.7	8.6	0.9	1.0

	Expected composition (At. %) – Calculated values <sup>b</sup>					
	O 1s	N 1s	C 1s	Cl 2p	P 2p	Na 1s
Liposome	10.1	5.3	79.8	3.4	1.4	0
siLex	10.2	5.3	79.7	3.4	1.4	0
Nalg-siLex	11.8	4.8	78.4	3.5	1.3	0.3

<sup>a</sup> S was also detected in sodium alginate sample and represented 0.87% of atomic composition

<sup>b</sup> values are calculated from the values measured for the molecules alone (data at the upper part of the table) and taking into account the relative molar proportion of each molecule for the preparation of each particle as following, liposome: DMAPAP / DOPE, 1/1; siLex: DMAPAP / DOPE / siRNA, 12/12/0.1125; Nalg-siLex: DMAPAP / DOPE / siRNA / Alginate, 32.2/32.2/0.1125/6.945

These calculated values are an approximation since the calculation is carried out considering that all the constituents are fully exposed (homogeneously distributed) and detectable on the surface of the particles. Nevertheless, they show that (i) the expected contribution of siRNA is negligible (compare liposome and siLex) while that of alginate is visible but weak (compare liposome, siLex and Nalg-siLex), (ii) for the three types of particles, carbon is predominant, followed by oxygen and then nitrogen. The middle part of Table 2 gives the elemental composition of the surface of liposome and lipoplexes obtained from XPS analysis. For the three particles, the same hierarchy, as observed for calculated values, is maintained between atoms with closer percentages for oxygen and nitrogen. However, the data from the assay show differences from the expected data since the lipoplexes profiles are almost identical and slightly different from that of the liposome. It can be deduced that the addition of the anionic molecules, alginate and/or siRNA, to the liposome induces a modification of the surface of the particle. The atomic composition of the surface of the two types of lipoplexes, however, is not different.

We have next sought to identify specific binding energy (BE) values of C 1s and N 1s through deconvolution of their spectra. Carbon 1s and N 1s spectra of particles are shown in Fig. S1B (left and right panel, respectively). The specific values of each peak and sample are shown in Table S1 (supplementary data). Chemical structures of nanoparticles components and the color correspondence of carbon and nitrogen bonds with BE peaks are shown in Fig. S1A. As for the previous analysis, we first identified the distribution of the binding energies of the molecules assayed separately (Table 3, upper part and supplementary data, Table S1, upper part), then of the three types of particles (Table 3, middle part and supplementary data, Table S1, lower part), and calculated the expected repartition of binding energies (Table 3, lower part) from the data obtained with molecules assayed separately following the same strategy as for atomic composition. Concerning the analysis of the N 1s signal, only the values for DMAPAP and siRNA are indicated in Table 3 since alginate does not contain any nitrogen and the N 1s signal of DOPE is very weak, this molecule containing only one nitrogen atom. The results obtained for the components alone are in agreement with the structure of these molecules. Unlike the previous surface elemental composition analysis (Table 2), the results obtained from the measured data are very different from the expected values obtained by calculation, which suggests that the molecules organize themselves within the particles to produce a surface in which only a part of the molecules is visible. With regard to liposome, this is consistent with what is known about the organization of cationic lipid molecules in a liposome-like structure: lipids form a continuous bilayer in which lipid molecules are packed with their hydrophobic tails pointing inwards and their hydrophilic heads outward, exposed to water. This specific organization of amphiphilic molecules in an aqueous medium explains the significant difference between the measured and calculated distributions of the C 1s bonds observed for liposomes. C-C bonds represent only 25.6 % of the detectable surface linkages of the liposomes whereas they should be very predominant (73 %) if they were visible. The surface of liposomes exhibited a large number of C-O/C-N (65%) and amide/amine nitrogen (91%) bonds, which are mainly found in the head region of the lipids. This result indicates that their surface is predominantly covered by the polar head of lipids and is in agreement with the global positive charge brought by the cationic lipid DMAPAP detected in the  $\zeta$  potential measurement of liposomes (+ 90 mV). With regard to N 1s, the measured values also differ from the calculated expected values, in particular the percentage of N-C bonds, much lower than the expected value (44%). Since the nitrogen molecules are located exclusively in the polar head of the lipids, this difference suggests that the organization of the polar heads is such that the whole of this portion of lipid is not accessible to the analysis.

**Table 3**

C and N surface species calculated or obtained by deconvolution of C 1s and N 1s spectra of molecules and particles (lipoplexes +/- R of 8).

Sample	% Concentration – from deconvolution of measured data							
	C 1s				N 1s			
	C-C	C-O / C-N	C=O	COO	N-C	NH <sub>2</sub> / NH <sub>3</sub>	NHCO	
DMAPAP	87.4	8.2	4.5		43.7	49.9	6.4	
DOPE	58.1	30.5	8.8	2.6				
siRNA	47.7	46.3	6.0		55.8	41.3	2.9	
Alginate	5.3	55.5	24.3	15.0				

	% Concentration – from deconvolution of measured data							
	C 1s				N 1s			
	C-C	C-O / C-N	C=O	COO	N-C	NH <sub>2</sub> / NH <sub>3</sub>	NHCO	N <sup>+</sup> -PO <sub>4</sub> <sup>3-</sup>
Liposome	25.6	65.5	6.8	2.2	8.9	56.7	34.3	
siLex	9.0	73.2	14.8	3.0	5.3	34.7	51.9	8.1
Nalg-siLex	22.2	62.4	13.4	2.0	10.9	41.7	47.4	

	Expected % Concentration – Calculated values <sup>a</sup>						
	C 1s				N 1s		
	C-C	C-O / C-N	C=O	COO	N-C	NH <sub>2</sub> / NH <sub>3</sub>	NHCO
Liposome	72.8	19.4	6.7	1.3	43.7	49.9	6.4
siLex	72.6	19.5	6.6	1.3	43.8	49.8	6.4
Nalg-siLex	66.2	22.9	8.4	2.6	43.7	49.9	6.4

<sup>a</sup> values are calculated from the values obtained for the molecules alone (data at the upper part of the table) and taking into account the relative molar proportion of each molecule for the preparation of each particle as following, liposome: DMAPAP / DOPE, 1/1; siLex: DMAPAP / DOPE / siRNA, 12/12/0.1125; Nalg-siLex: DMAPAP / DOPE / siRNA / Alginate, 32.2/32.2/0.1125/6.945

According to the calculated expected values, the contribution of siRNA is negligible on the distribution of the C 1s and N 1s bonds, and that of alginate is weak but visible for C 1s bounds. The measured data first show that, as for the liposome, the proportion of detectable C-C bonds on the surface of lipoplexes (siLex and Nalg-siLex) is much lower than expected, indicating that the lipid tails are masked, probably within the lipid bilayer, originate from liposome, that would remain after the addition of anionic molecules. In addition, the measured data shows that the addition of siRNA significantly alters the surface of the particle, as evidenced by the distribution of the C 1s bonds and, to a lesser extent, that of the N 1s bonds. In particular, compared to the liposome, in siLex there is a clear decrease in the percentage of C-C bonds and an increase in C-O / C-N and C=O bonds, as well as a reversal in the NHCO and NH<sub>2</sub>/NH<sub>3</sub> bond hierarchy. Since BE peak at 286 eV in C 1s spectrum represents either C-O or C-N species, the BE reduction of N-C in the N 1s spectrum indicated that the rise of this BE value concerns mostly C-O species, which are found in the ribose ring of siRNA and in the linker domain of DOPE. We can also note the presence of an unexpected peak at 404.1 eV in the N 1s region of siLex, a peak whose binding energy could be attributed to a N<sup>+</sup>-PO<sub>4</sub><sup>3-</sup> bond (see discussion part). As for the liposome and siLex, the measured data from the deconvolution of the N 1s and C 1s spectra of Nalg-siLex differ from the calculated expected data; they also differ from the

measured data of siLex, especially concerning the carbon bonds, and are closer to those of the liposome. The N 1s profile of Nalg-siLex remains close to that of liposome and / or siLex, except that unlike siLex, the peak at 404.1 eV is not detected.

Globally, the spectra deconvolution shows that there were some differences between the surface compositions of the two types of lipoplexes, especially for nitrogen species. Because of the complexity of the objects studied here, it is difficult to interpret quantitatively the surface modifications occurring upon the formation of lipoplexes. In particular, none of the molecules composing lipoplexes contains an atom that made it possible to differentiate it from other molecules. It was therefore not possible to determine quantitatively which molecule or part of a molecule was present on the surface of the particle. However, one can state that a strong reorganization took place revealing new surface contributions when siRNA or siRNA + alginate are mixed with cationic liposome and that siLex and Nalg-siLex exhibited notable difference on their surface.

#### *3.4. Structural study – SAXS*

The lipid structural characteristics of liposome and lipoplexes suspensions were also evaluated by SAXS. Fig. 4 shows DMAPAP/DOPE (1:1, M:M) liposome suspension scattering profiles. The liposome suspension prepared in NaCl 150 mM presented two major reflections, named  $L_1$  ( $0.73 \text{ nm}^{-1}$ ) and  $L_2$  ( $1.40 \text{ nm}^{-1}$ ), representing a lamellar phase with Q value ratio of 1:2 and a lattice spacing of 8.61 nm. The apparent strong intensity of the  $L_2$  reflection with respect to the  $L_1$  reflection and the detection of a third broad peak evidence the coexistence of a second structural phase. A fitting curve of cationic liposomes at 1 mM (inset in Fig. 4) displays, beyond lamellar phase, two broad peaks with a ratio of 1: $\sqrt{2}$  typical of cubic phase ( $C_1$  peak at  $1.32 \text{ nm}^{-1}$  and  $C_2$  peak at  $1.90 \text{ nm}^{-1}$ ). This phase presents a lattice spacing of 4.76 nm. The area below each fit component is directly proportional to its phase volume, while the domain size ( $L$ ) is inversely proportional to the peak width  $\Delta Q$ , following the relation  $L = 2\pi/\Delta Q$ . In this case, the fitting of the experimental data indicates that cubic phase volume is approximately 30-40% larger than the volume of lamellar phase, with average domain sizes of 20 and 9 nm, respectively. Such sizes are compatible with the coherent range of local molecular packing registry observed by TEM (Fig. 3). The observed pattern of Bragg peaks remains the same, independently of liposome concentration, within the evaluated range depicted in Fig. 4.

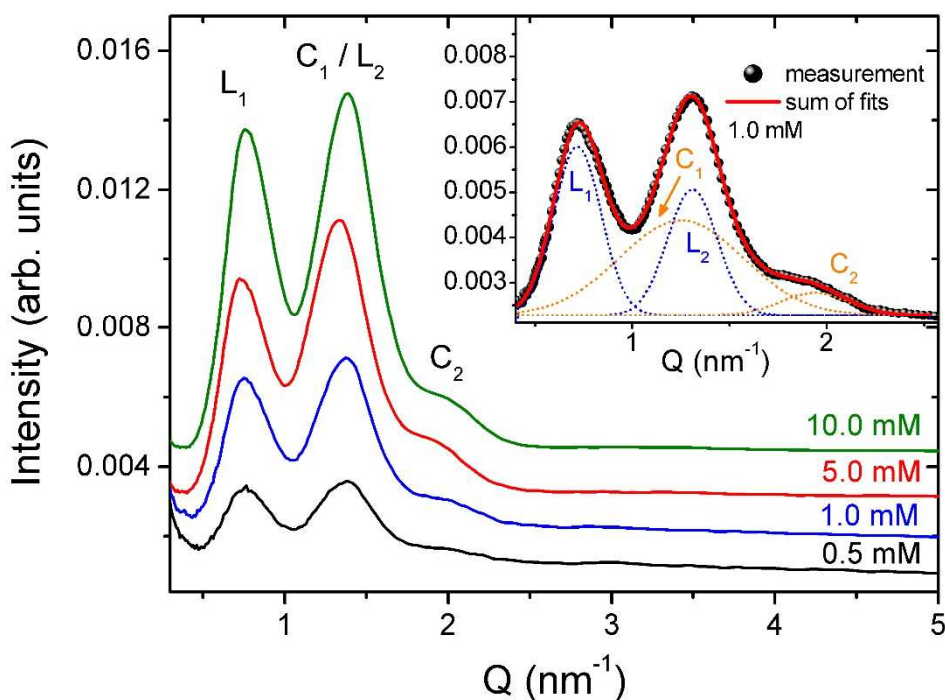


**Fig. 4.** SAXS profiles of cationic liposome suspension (DMAPAP:DOPE 1:1 in NaCl) at different concentrations. Inset: fitting of the 1.0 mM curve, depicting peak values for the liposome suspension. The retrieved peak positions are:  $L_1$  at  $Q = 0.73 \text{ nm}^{-1}$ ;  $L_2$  at  $Q = 1.40 \text{ nm}^{-1}$ ;  $C_1$  at  $Q = 1.32 \text{ nm}^{-1}$ ;  $C_2$  at  $Q = 1.90 \text{ nm}^{-1}$ . Other concentrations present similar profile and peak position ratios.

The SAXS profiles of siLex and Nalg-siLex are shown in Fig. 5A and B, respectively. siLex and Nalg-siLex were evaluated at  $\pm R$  of 1, condition in which it is expected that all cationic lipid is completely complexed, forming neutral lipoplexes. SAXS profiles from siLex suspension at this  $\pm R$  showed a single sharp reflection at  $Q$  value of  $0.95 \text{ nm}^{-1}$  which is considered as a typical lamellar phase with lattice spacing of  $6.61 \text{ nm}$ , called  $L_1$  (black line, Fig. 5A). The absence of a second reflection indicates that this phase presents only short range order, suggesting that siLex dispersion is partially organized in lamellar structures surrounded by non-ordered or poorly ordered lipoplexes. In the case of Nalg-siLex at the same  $\pm R$ , the  $L_1$  reflection seems to be merged with an additional reflection indicated by an arrow (green arrow, Fig. 5B). Again, as for siLex, the absence of a second reflection indicates that Nalg-siLex possess a short range order. Analysis of siLex at  $\pm R$  of 8, condition in which there is an excess of cationic lipid over siRNA, compared to lipoplexes at  $R \pm 1$ , present a more complex SAXS profile. As shown in Fig. 5A (red line), the  $L_1$  reflection typical of siLex at charge ratio 1 is still marked. Three additional major reflections were detected at  $Q$  values of  $0.83$ ,  $1.20$  and  $1.92 \text{ nm}^{-1}$ . The  $Q$  values ratios indicate that, in addition to the lamellar phase ( $L_1$ ,  $L_2$ ), part of siLex is organized in a cubic phase ( $C_1$ ,  $C_2$ ) and both are distinct from the lamellar and cubic phases of liposomes (dotted line, Fig. 5). In these conditions the cubic phase presents a lattice spacing of  $7.57 \text{ nm}$ , while the lamellar phase keeps its lattice spacing of approximately  $6.6 \text{ nm}$ . The presence of  $L_2$  reflection at  $Q$

value of  $1.92 \text{ nm}^{-1}$  could be attributed to the formation of a long range order lamellar phase, unlike siLex at  $R \pm 1$  (with respect to the black curve of Fig. 5A).

The Nalg-siLex SAXS profile presents peaks at similar  $Q$  values as siLex, but they are wider than the observed reflections for siLex (red line, Fig. 5B). There is a slight shift of the  $L_1$  peak towards  $1.01 \text{ nm}^{-1}$ , representing a small lattice spacing contraction of this phase, from 6.6 to 6.22 nm. On the other hand,  $C_1$  peak remains at  $0.83 \text{ nm}^{-1}$ , keeping the cubic phase lattice spacing of 7.57 nm. The width of reflections leads to the merge of  $C_1$  and  $L_1$  peaks into a single large peak, preventing the precise determination of  $Q$  values. In all analysis with  $\pm R$  of 8 it was not possible to fit the profile with a simple peak combination (as in the inset of Fig. 4), due to the presence of a diffuse background below all peaks, most probably due to first-neighbor distances of a fraction of the constituents with some degree of amorphization (no short- or long-range order). Indeed, simple fitting procedures were no longer reliable since they would ignore the diffuse data, producing an overestimation or underestimation of phase volumes. In this sense, the SAXS profiles from Fig. 5 with  $R \pm 8$  differ considerably from the profiles shown in Fig. 4, requiring about 6 ~ 8 peaks to produce a good fit. We decided then to skip such fitting procedures, which are unable to add quantitative information to our discussion.

We also tried to increase the intensity of peaks (and therefore the volume of ordered structures) preparing both lipoplexes at the same charge ratio ( $\pm R$  of 8) and twice as concentrated (blue lines, Fig. 5). Analysis of siLex prepared at this condition showed that reflections  $C_1$  and  $L_1$  merged and  $L_2$  was no longer detected. Moreover, the vicinity of the  $C_2$  reflection presents a hump shape at high  $Q$  values which possibly contains overlapped reflections. In the case of Nalg-siLex, the increase of lipoplexes concentration results in a reflection pattern which is similar to that of the more diluted suspension, with more intense peaks and better detection of  $L_1$ . For both concentrations assayed, the presence of alginate in lipoplexes (Nalg-siLex) leads to a slight difference in the relative proportion of the two observed cubic and lamellar structures, compared to siLex.

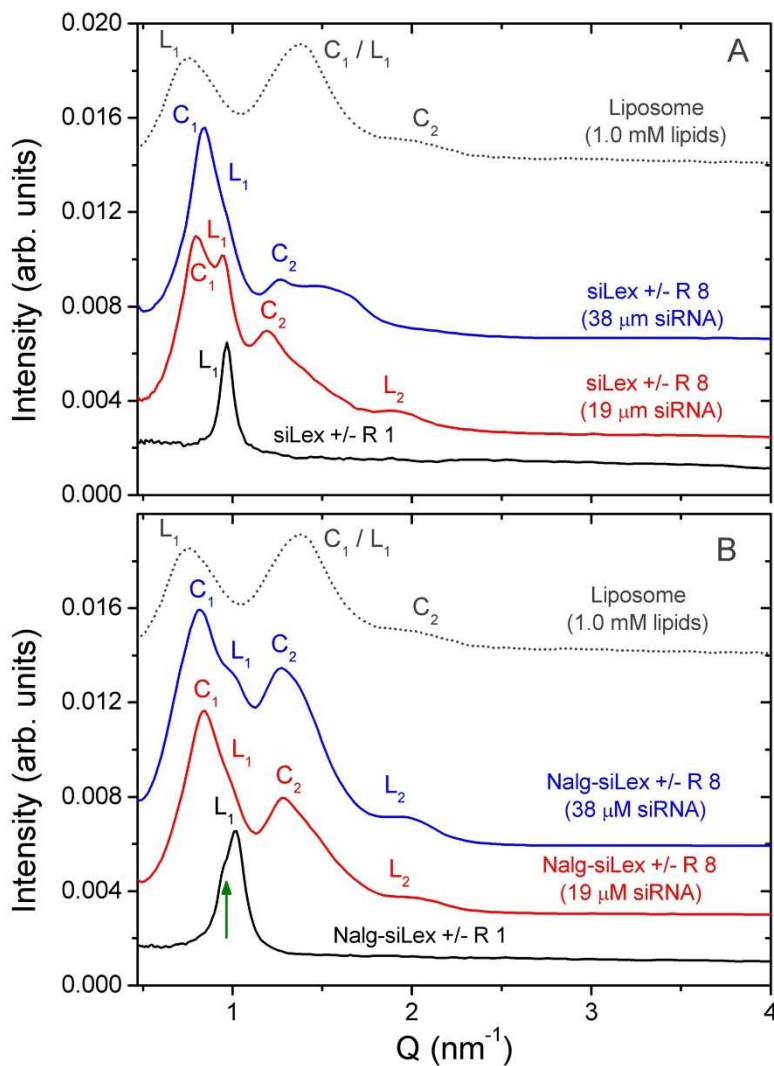


**Fig. 5.** SAXS profiles of siLex (A) and Nalg-siLex (B) suspensions in NaCl 150 mM at +/- R of 1 (black line: 19 $\mu$ M siRNA) or 8 (red line: 19 $\mu$ M siRNA, blue line: 38 $\mu$ M siRNA) and cationic liposome suspension in H<sub>2</sub>O at 1 mM lipid (dotted line). Green arrow, additional reflection (see in text).

Taken together, results from XPS and SAXS analysis show that there are differences between siLex and Nalg-siLex. These differences, however, remain modest and mainly concern the surface of the particles as well as, to a lesser extent, their internal structure.

### 3.5. *In vitro* cytotoxicity and gene efficiency, and *in vivo* toxicity

Nalg-siLex comprising 2.7 times more lipids in their composition than siLex (as pointed out in §2.2 and §3.1), we have also studied the possible toxicity induced by the application of these particles to cultured cells or systemic administration to mice. We compared the cellular toxicity induced on mouse melanoma B16 cells by the two types of lipoplexes prepared at +/- R 8 and at increasing concentrations of siRNA (Fig. 6A). We observed that more than 75 % of cell viability is maintained for

siRNA concentrations up to 40 nM, with a value for IC50 around 100 nM. No significant difference between the two types of particles is observed. In parallel, we explored the gene silencing activity of luciferase-targeted siRNA lipoplexes using B16 cells that constitutively express luciferase gene (B16-Luc). siLex and Nalg-siLex, prepared at +/- R of 8 were applied to B16-Luc at increasing final siRNA concentration, from 8.5 to 50 nM to evaluate their gene silencing efficiency. As shown in Fig. 6B, Nalg-siLex was significantly more efficient than siLex in the concentration range tested. To obtain, with siLex, the same gene silencing efficacy as with Nalg-siLex, it is necessary to use a concentration of siRNA at least twice as high. This difference is no longer observable for the highest concentrations of siRNA because the system saturates (data not shown). The gene silencing of siLex and Nalg-siLex is specific since no inhibition was detectable when a non-specific control siRNA was used, regardless of the condition (data not shown). To find out if the higher efficiency of Nalg-siLex is due to a potential action of alginate on the cytoplasmic RNAi machinery, we evaluated the efficiency of siLex (containing luciferase-specific siRNA) when it is complemented by either Nalg-siLex\* or siLex\* particles containing the non-specific control siRNA. Sodium alginate is thus introduced into the cell within a particle without effectiveness on the activity of luciferase since it contains a control siRNA. As shown in Fig. 6C, the presence of alginate in the complementation particle has no effect on the efficiency of the particle.

We then addressed the issue of *in vivo* toxicity. siLex and Nalg-siLex were injected i.v. to mice. It is known that the systemic administration of siRNA formulations to mice can lead to a detectable and transient elevation in serum inflammatory cytokines within 1-2 hours that is typically resolved within 12-24 hours after treatment. In this work, siLex and Nalg-siLex or glucose were injected to mice and serum was harvested at 2 h, 6 h or 24 h post-injection. Twenty-four hours after the injection all mice exhibited normal behavior and no visible sign of toxicity (ruffled fur, reluctance to move, ...). Cytokines (TNF- $\alpha$ , INF- $\alpha$ , IFN- $\beta$ , INF- $\gamma$  and IL-6) were assayed. No elevation of these cytokine concentrations was detectable in sera collected 2 h or 24 h after injection.

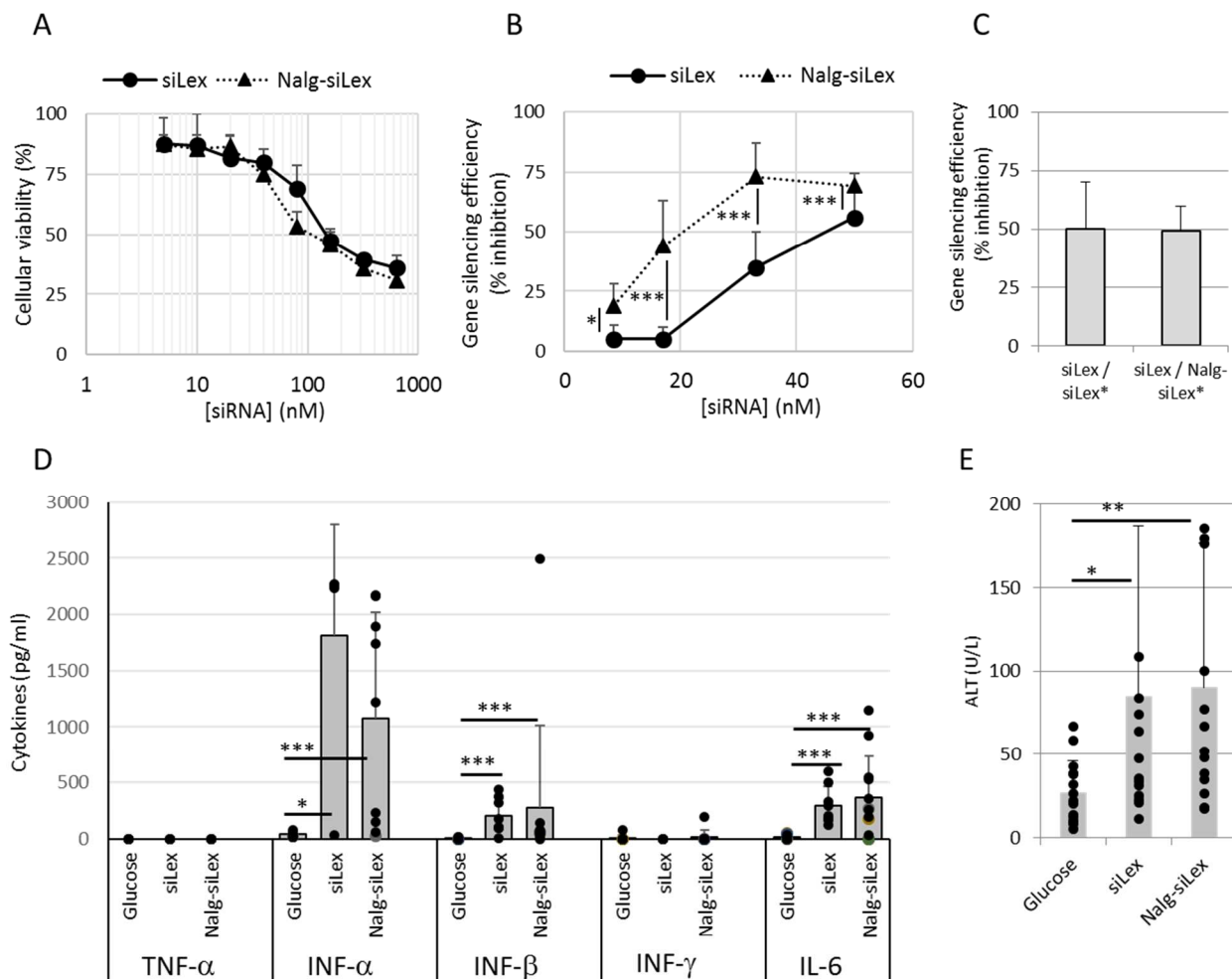


**Fig. 6.** Assessment of *in vitro* toxicity and gene silencing efficiency, and *in vivo* toxicity. (A) Cellular viability of B16 cells transfected for 24 h with lipoplexes prepared as increasing concentrations of siRNA was evaluated with MTT assay. (B-C) Gene knockdown of luciferase activity in B16-Luc with siLex and Nalg-siLex prepared at +/- R of 8 with (B) 8.5, 17, 33 and 50 nM siRNA anti-luciferase as indicated, (C) 33 nM and supplemented with siLex\* or Nalg-siLex\* prepared at the same conditions but with siRNA control. (B-C) Inhibition of luciferase activity was expressed as a percentage of luciferase activity of non-transfected cells. Means and standard deviations of the means were calculated from 3 independent experiments, each condition performed in triplicate in each experiment. (D-E) siLex, Nalg-siLex (1 mg/kg) or glucose were i.v. injected to mice. (D) Mean concentration of TNF- $\alpha$ , INF- $\alpha$ , INF- $\beta$ , INF- $\gamma$  and IL-6 obtained at 6 h following injection were assayed in serum. (E) 24 h after injection, ALT was assayed in serum. Means and the standard deviations of the means were calculated from 6 to 9 replicates of different mice (\* 0.01 < p < 0.05; \*\* 0.005 < p < 0.01; \*\*\* p < 0.005). Means are symbolized by the gray bars and dots represent the individual values of each sample.

Six hours after particles injection (Fig. 6D), detectable levels of INF- $\alpha$ , INF- $\beta$  and IL-6 were observed, whereas no elevation of TNF- $\alpha$  or INF- $\gamma$  concentration was detectable. The addition of sodium alginate did not change the cytokine level induced by the particle injection. We also assayed Alanine Aminotransferase (ALT) in sera 24h post-injection to investigate the lipoplexes-induced hepatotoxicity. Again we observed some moderate increase of ALT level induced by siRNA lipoplexes injection but no difference between siLex and Nalg-siLex (Fig. 6E).

In conclusion, the presence of sodium alginate in siRNA lipoplexes did not significantly modify the mild cytokine induction and hepatotoxicity usually observed upon injection to mice of siRNA-containing particles and Nalg-siLex can be applied to mice without evidence of toxicity.

#### 4. Discussion

The purpose of this work is to explore the impact of adding alginate to lipoplexes by premixing it with siRNAs. We chose to premix siRNA and alginate before adding cationic liposomes, assuming that this homogeneous mixture would generate particles with a homogeneous relative proportion of these two components. However, another possibility could be considered, which would be to add the three components (siRNA, alginate and cationic liposome) in one step. Particles of modified structure and / or increased activity could be obtained. It would be then necessary to control the conditions of mixing, for example thanks to microfluidic technology. Different characteristics of lipoplexes prepared without (siLex) or with alginate (Nalg-siLex) were compared along the previous section. However, a straightforward comparison cannot be directly made, since one must fix the final amount or concentration of siRNA, which is the active ingredient, and also to fix the +/- charge ratio, which largely determines the characteristics of the obtained particles. It was then mandatory to choose a +/- charge ratio of 8, which allows the formation of particles whose sizes are compatible with *in vivo* administration. For each analysis method described in the previous paragraphs, we compared then particles with the same final amount of siRNA. On the other hand, this choice requires a comparison among particles which do not present the same final amount of lipids since Nalg-siLex contain 2.7 times more lipids than siLex. Such interplay of variables must be kept in mind for the discussion that follows.

We first showed that the addition of alginate does not modify the size or the  $\zeta$  potential of the particles, nor the capacity of the cationic lipid to complex siRNA, even if the size analysis suggests that siLex are more polydisperse than Nalg-siLex. This could indicate that alginate contributes to better organization of components, as well as for Nalg-siLex homogeneity. In addition, we have previously shown, using an electrophoretic technique, that alginate is associated with the particle (additional data of [7]).

The morphology of siLex and Nalg-siLex obtained through transmission electron microscopy (TEM) showed that both types of lipoplexes present multilamellar structures. Numerous articles have described the appearance of lipoplexes, prepared either with plasmid DNA or with siRNA, in TEM studies. Heterogeneous particles with shapes varying from stacks of bilayers (flat, concentric or bent) to amorphous aggregates with partially lamellar structures have been reported [26-28]. This multilamellar internal structure is often described as lipid bilayers interacting with coating nucleic acids resulting in a particulate system, which is the case for the two types of particles studied here. However, the addition of alginate seems to give rise to different lamellae arrangement, suggesting

the observation of a distinct organization, if not a different structure. In addition, Nalg-siLex have a smoother appearance than siLex, which led us to better characterize the surface of these particles.

We used X-ray photoelectron spectroscopy to compare the surface of the particles. To our knowledge, this technique has never been used to study the surface of lipoplexes. We first examined surface properties resulting from the XPS spectrum of the liposome, formed by equimolar amount of cationic lipid DMAPAP and zwitterionic lipid DOPE, to ensure that this technique could be applied to the characterization of the surface of lipid-based particles. The distribution of detectable chemical bonds at the surface of the liposome, derived from the deconvolution of the C 1s and N 1s spectra, is compatible with the supramolecular formation of a lipid bilayer, typical of liposomes, indicating that despite the drying step undergone by the liposome suspension, the organization of the amphiphilic lipids generated to protect the hydrophobic domain from the aqueous environment is preserved. In siLex, the relative proportion of siRNA with respect to lipids is very low (see values in Table 2), yet the addition of siRNA to liposome to form lipoplex, induces a significant modification of the surface of the obtained particle. This observation also helps to validate the use of XPS to characterize lipoplexes surface. Our goal was to compare the surface characteristics of siLex and Nalg-siLex. It is found that Nalg-siLex surface chemical composition resembles more the liposome than the surface of siLex. In particular, deconvolution of the N 1s spectrum reveals the presence of an atypical peak only in siLex. This peak at 404.1 eV (not detectable on the surface of Nalg-siLex) is not usually retrieved in organic nanoparticles and could indicate the presence of the cationic nitrogen of DMAPAP in a particular environment, possibly interacting electrostatically with phosphate groups of siRNA. This result is in agreement with the intercalation of siRNA molecules between the lipid bilayers of liposomes. Given that Nalg-siLex contains 2.7 times more lipids than siLex it cannot be completely ruled out that this peak is also present in Nalg-siLex, but masked by the presence of larger amounts of lipids. However, this result suggests the presence of a chemical binding that could be related to the interaction of siRNA with cationic lipid, detectable in siLex and not in Nalg-siLex surface. Since we compared particles prepared with the same final amount of active ingredient, siRNA, the comparison is relevant and this observation could explain the superior ability of Nalg-siLex to preserve the siRNA integrity. In this scenario we consider that the amount of additional lipid present in Nalg-siLex prevents the detection of this interaction using XPS and could, in the same way, make the siRNA / cationic lipid interaction inaccessible to potential competitors present in biological media.

We also compared the internal structure of siLex and Nalg-siLex using a widely described method: synchrotron radiation SAXS analysis. We first identified the structure adopted by DMAPAP / DOPE liposome as a reference. This structure, was measured at equivalent systems published previously

(where lamellar, hexagonal or cubic structures were found, according to composition of systems [17, 29-31], and the condition adopted by our system was directly measured. As shown in Fig. 4, DMAPAP/DOPE liposomes present a coexistence of lamellar and cubic phases. According to the “ideal” sequence of phases proposal for amphiphilic molecule aggregates in aqueous solution such as phosphatidylethanolamine (PE) and phosphatidylcholine (PC) lipids, the cubic phase is a mesophase formed during the typical transition of lamellar to hexagonal phases [32]. As reviewed by Koynova and Tenchov [33], diacyl or dialkyl phospholipids and glycolipids that have chain lengths of C14 or shorter tend to form inverted cubic phase while longer-chain lipids present direct lamellar-inverted hexagonal phase transitions. A recent study of the same authors evaluated some parameters that induce the conversion of the lamellar  $L\alpha$  phase into cubic phases of PE lipid dispersions [34]. Among them, the presence of small amounts of charged lipid admixtures and some solutes such as sodium salts and saccharides, facilitates the formation of cubic phase for some PE lipids studied. Additionally, the PE dispersions at concentration below 20–25 wt % of lipid concentration form pure cubic phases by T-cycling around 25-80 °C depending on the evaluated lipid. The exposure of pure DOPE dispersion to several repeated temperature cycles is one of long-time strategies studied to generate typical cubic phase reflections by X-ray small-angle diffraction pattern [35-36]. These results show that the occurrence of DOPE cubic phases takes place after subjecting the samples to several thermal cycles across the L → H transition between -5 °C and 15 °C. Koynova et al. [37] reported that a specific cationic lipid dispersion, derived from PC lipid, is able to form coexisting lamellar and cubic phases at room and physiological temperature. In this work, we prepared DMAPAP/DOPE liposomes in equimolar ratio of C14 cationic lipid and C18 zwitterionic lipid, respectively, at highly diluted (3.2 wt % lipid) NaCl 150 mM aqueous solution and the coexistence of lamellar and cubic phases is therefore not surprising. In addition, even if we did not submit DMAPAP/DOPE liposomes to intentional T-cycling at high temperatures, we must take into account that our liposome dispersion is stored at 4 °C and all sample preparation and analyses were made at room temperature. Then, as described before, this variation of storage and analysis temperatures could also be a factor which leads to the formation of coexisting lamellar and cubic phases. In this work, we aimed to compare the differences between lipoplexes prepared with and without alginate and evaluated liposome internal organization as a reference. However, a systematic study of DMAPAP/DOPE liposome by varying the relative proportions of the two lipids could be considered in future work to understand how to obtain selectively lipid nanoparticles with a particular structure.

The SAXS profile of siLex and Nalg-siLex prepared at +/- R of 8 were complex and the study of both types of lipoplexes at +/- R of 1 was required as a condition for which as many positive as negative

charges are brought, by assuming that the structure would be simpler. The SAXS spectra of siLex and Nalg-siLex at +/- R of 1 showed a single reflection named  $L_1$  (Fig. 5) which was attributed to a lamellar phase. The Q value of this reflection (around  $1 \text{ nm}^{-1}$ ) is very close to that reported for the lamellar phase of related lipoplexes [17, 31]. However, the wider  $L_1$  reflection of Nalg-siLex suggests that the inclusion of alginate induces the formation of lipoplexes with distinct anionic components distribution resulting in structures with different domain sizes or even a phase transition between them. The absence of a second reflection indicates that Nalg-siLex possess a short range order as well as siLex. According to the predictions of theoretical aggregation-disaggregation model [38], cationic lipid-DNA complexes at isoneutrality form clusters of lipoplexes due to the aggregation of particles. At this condition, siLex and Nalg-siLex form large visible precipitates, in agreement with these theoretical results. At +/- R of 8, siLex and Nalg-siLex showed the coexistence of lamellar and cubic phases. For both lipoplexes, a second lamellar reflection named  $L_2$  is detected indicating that structures are more organized than those at +/- R of 1 (red lines, Fig. 5A and 5B). Furthermore, the respective intensity of lamellar and cubic phases detected for both lipoplexes indicates that the addition of alginate prompts the predominance of a cubic phase in Nalg-siLex, while lamellar phase is more evident in siLex suspension. In order to increase the peak intensity of SAXS profiles, lipoplexes were prepared twice as concentrated (blue lines, Fig. 5). In the case of siLex,  $C_1$  and  $L_1$  reflections merged and a great hump appeared next to  $C_2$  reflection which could be attributed to the formation of other lipid structures or a volume of amorphous material. Furthermore, the observed changes in peak intensity suggest that there is an increase of cubic phase volume and a decrease of lamellar phase volume of lipoplexes. Regarding to Nalg-siLex, the increase in concentration did not seem to affect the relative proportion of the two phases, lamellar and cubic. Through the comparison of SAXS profiles of both types of lipoplexes dispersions at different concentrations and +/- R of 8, it seems that the addition of alginate favors the coexistence and stability of lamellar/ cubic phases, which keep their approximate volume proportion, while the siLex dispersion modifies the measured profile, leading to the emergence of additional (and distinct) structural organization.

In most articles in the literature, samples used in SAXS analyses are made at low water content, allowing the detection of defined and sharp phase reflections and easy result interpretations. However, lipid concentrations commonly used in biological assays are far from the conditions used in SAXS analyses, in particular because of the high cytotoxicity induced by high lipid content [17, 30]. Therefore, we decided to evaluate the structures of our lipid nanoparticles prepared as more diluted dispersions. At these conditions, the results of SAXS experiments revealed broad peaks, consistent with the fact that the samples were prepared in more than 90 % water, even for the most concentrated lipoplexes dispersions used in this work. Previous reports showed that the dilution of particles prepared with mixtures of cationic lipid and cubic phase-forming lipids (0.02 wt % in

optiMEM) modifies SAXS profiles, revealing only the first two reflections of the cubic phase detected in the same sample at higher concentration [30]. The authors showed that in diluted conditions, peaks in SAXS spectra are broad due to small domain size of phases, which is consistent with our results presented in Fig. 5. In addition, since we studied lipoplexes prepared at +/- R of 8, that is to say in the presence of an excess of lipids with respect to the anionic molecules, lipids which are not incorporated into lipoplexes could be considered as another factor that broadens the detected reflections due to the formation of different coexisting and less organized structures.

Cell studies have shown that while containing more lipids, which is potentially cytotoxic, Nalg-siLex do not induce more toxicity than siLex, while exhibiting a significant increase in gene silencing efficiency. This increase in efficiency is not due to an effect of alginate on RNAi machinery (Fig. 6C). The induction of inflammatory cytokines observed in the serum of injected mice is probably due to the known activator effect of siRNAs. Indeed, nucleic acids are key structures sensed by the innate immune system, which comprises the cells and mechanisms that defend the host from infection by other organisms in a non-specific manner [39]. The corresponding receptors for foreign nucleic acids include members of Toll-like receptors (TLR), RIG-I-like receptors, and intracellular DNA sensors [40-41]. However, the administration of Nalg-siLex does not induce more inflammatory cytokine production than that of siLex.

## 5. Conclusion

In this study, we subjected the siRNA lipoplexes prepared with sodium alginate (Nalg-siLex) to extensive characterization using complementary methods for advanced analysis of the surface and structure, comparing them to vectors without anionic polymer (siLex). Notably, we have used XPS to compare the surface of both type of lipoplexes and identified, on the surface of conventional lipoplexes (siLex), an unusual peak in the N 1s region that could indicate the presence of the cationic nitrogen of DMAPAP, possibly interacting electrostatically with phosphate groups of siRNA. This peak was not observed in Nalg-siLex, suggesting that siRNA is less exposed in these innovative lipoplexes. The structure characterization by SAXS showed that both lipoplexes presented lipid organization as coexisting lamellar and cubic phases, but in different ratio of each one. The inclusion of alginate seems to maintain the lipid phase ratio independently of suspension concentration. These findings are in accordance with the TEM images and size distribution of siLex and Nalg-siLex which show distinct microscopic aspect and better homogeneity of Nalg-siLex. Although requiring the addition of more lipids for their preparation, these particles do not exhibit more toxicity on cells or in animals than particles without alginate, while having a much higher *in vitro* gene silencing efficiency. The addition of alginate makes it possible to obtain a siRNA delivery vector compatible with *in vivo*

administration, which is more stable and more effective than the initial vector (without alginate). We have already demonstrated the effectiveness of these particles in two animal models, chick embryo [42] and mouse (supplementary data Fig. S2). Thanks to this inexpensive, non-toxic and biocompatible molecule, it is easy to increase the stability and effectiveness of lipoplexes.

### **Acknowledgments**

Financial support was by CNPq, CAPES, COFECUB, FAPEMIG, CNRS, INSERM and Paris Descartes University. We acknowledge SOLEIL for provision of synchrotron radiation facilities and we would like to thank Javier PEREZ and Youssef LIATIMI for assistance in using beamline SWING. We are also grateful to ESRF (Grenoble, France) and the members of beamline ID02, especially Theyencheri NARAYANAN, for giving us access to the beamline, which allowed us to carry out the preliminary experiments necessary to develop the following tests. We are grateful to René LAI-KUEN for technical assistance in TEM and to the Microscopy Platform (TEM) and the Animal Platform (*in vivo* experiments), CRP2 -UMS 3612 CNRS -US25 Inserm-IRD –Faculté de Pharmacie de Paris, Université Paris Descartes.

## References

- [1] A. Fire, S. Xu, M.K. Montgomery, S.A. Kostas, S.E. Driver, C.C. Mello, Potent and Specific Genetic Interference by Double-Stranded RNA in *Caenorhabditis elegans*, *Nature* 391 (1998) 806-811.
- [2] M.L. Bobbin, J.J. Rossi, RNA Interference (RNAi)-based Therapeutics: Delivering on the Promise?, *Annu. Rev. Pharmacol. Toxicol.* 56 (2016) 103-122.
- [3] R. Titze-de-Almeida, C. David, S.S. Titze-de-Almeida, The Race of 10 Synthetic RNAi-Based Drugs to the Pharmaceutical Market, *Pharm. Res.* 34 (2017) 1339-1363.
- [4] C. Lorenzer, M. Dirin, A.M. Winkler, V. Baumann, J. Winkler, Going Beyond the Liver: Progress and Challenges of Targeted Delivery of siRNA Therapeutics, *J. Control. Release* 203 (2015) 1-15.
- [5] Y. Wang, L. Miao, A. Satterlee, L. Huang, Delivery of Oligonucleotides with Lipid Nanoparticles, *Adv. Drug Deliv. Rev.* 87 (2015) 68-80.
- [6] L. Weijun, F.C. Szoka Jr, Lipid-based Nanoparticles for Nucleic Acid Delivery, *Pharm. Res.* 24 (2007) 438-449.
- [7] A. Schlegel, C. Largeau, P. Bigey, M. Bessodes, K. Lebozec, D. Scherman, V. Escriou, Anionic Polymers for Decreased Toxicity and Enhanced in Vivo Delivery of siRNA Complexed with Cationic Liposomes, *J. Control. Release* 152 (2011) 393-401.
- [8] V. Escriou, P. Bigey, D. Scherman, Vectors Including an Anionic Macromolecule and a Cationic Lipid for Delivering Small Nucleic Acids, *European Patent EP 2389158 B1* (2009).
- [9] M.C. Hamoudi, E. Henry, N. Zerrouk, D. Scherman, P. Arnaud, E. Deprez, V. Escriou, Enhancement of siRNA Lipid-based Vector Stability and siRNA Integrity in Human Serum with Addition of Anionic Polymer Adjuvant, *J. Drug Delivery Sci. Technol.* 26 (2015) 1–9.
- [10] S. Patnaik, M. Arif, A. Pathak, N. Singh, K.C. Gupta, PEI-Alginate Nanocomposites: Efficient Non-Viral Vectors for Nucleic Acids, *Int. J. Pharm.* 385 (2010) 194-202.
- [11] T. Li, G.D. Wang, Y.Z. Tan, H.J. Wang, Inhibition of Lymphangiogenesis of Endothelial Progenitor Cells with VEGFR-3 siRNA Delivered with PEI-Alginate Nanoparticles, *Int. J. Biol. Sci.* 10 (2014) 160-170.
- [12] K.L. Douglas, C.A. Piccirillo, M. Tabrizian, Effects of Alginate Inclusion on the Vector Properties of Chitosan-based Nanoparticles, *J. Control. Release* 115 (2006) 354-361.
- [13] N. Dan, D. Danino, Structure and Kinetics of Lipid-Nucleic Acid Complexes, *Adv. Colloid Interface Sci.* 205 (2014) 230-239.
- [14] K.K. Ewert, A. Zidovska, A. Ahmad, N.F. Bouxsein, H.M. Evans, C.S. McAllister, C.E. Samuel, C.R. Safinya, Cationic Lipid-Nucleic Acid Complexes for Gene Delivery and Silencing: Pathways and Mechanisms for Plasmid DNA and siRNA, *Top Curr. Chem.* 296 (2010) 191-226.

- [15] D. Belletti, M. Tonelli, F. Forna, G. Tosia, M.A. Vandellia, B. Ruozi, AFM and TEM Characterization of siRNAs Lipoplexes: A Combinatory Tool to Predict the Efficacy of Complexation, *Colloid. Surface. A* 436 (2013) 459–466.
- [16] S. Colombo, D. Cun, K. Remaut, M. Bunker, J. Zhang, B. Martin-Bertelsen, A. Yaghmur, K. Braeckmans, H.M. Nielsen, C. Foged, Mechanistic Profiling of the siRNA Delivery Dynamics of Lipid-Polymer Hybrid Nanoparticles, *J. Control. Release* 201 (2015) 22-31.
- [17] N.F. Bouxsein, C.S. McAllister, K.K. Ewert, C.E. Samuel, C.R. Safinya, Structure and Gene Silencing Activities of Monovalent and Pentavalent Cationic Lipid Vectors Complexed with siRNA, *Biochemistry* 46 (2007) 4785–4792.
- [18] G. Byk, D. Scherman, B. Schwartz, C. Dubertret, Lipopolyamines as Transfection Agents and Pharmaceutical Uses Thereof, US Patent 6171612 (2001).
- [19] H. Rhinn, C. Largeau, P. Bigey, R.L. Kuen, M. Richard, D. Scherman, V. Escriou, How to Make siRNA Lipoplexes Efficient? Add a DNA Cargo, *Biochim. Biophys. Acta* 1790 (2009) 219-230.
- [20] T. Tagami, J.M. Barichello, H. Kikuchi, T. Ishida, H. Kiwada, The gene-silencing effect of siRNA in cationic lipoplexes is enhanced by incorporating pDNA in the complex, *Int. J. Pharm.* 333 (2007) 62-69.
- [21] K. Bollérot, D. Sugiyama, V. Escriou, R. Gautier, S. Tozer, D. Scherman, T. Jaffredo, Widespread Lipoplex-Mediated Gene Transfer to Vascular Endothelial Cells and Hemangioblasts in the Vertebrate Embryo, *Dev. Dyn.* 235 (2006) 105-114.
- [22] C. Evora, I. Soriano, R.A. Rogers, K.N. Shakesheff, J. Hanes, R. Langer, Relating the Phagocytosis of Microparticles by Alveolar Macrophages to Surface Chemistry: the Effect of 1,2-Dipalmitoylphosphatidylcholine, *J. Control. Release* 51 (1998) 143-152.
- [23] M.Ø. Andersen, A. Lichawska, A. Arpanaei, S.M. Rask Jensen, H. Kaur, D. Oupicky, F. Besenbacher, P. Kingshott, J. Kjems, K.A. Howard, Surface Functionalisation of PLGA Nanoparticles for Gene Silencing, *Biomaterials* 31 (2010) 5671-5677.
- [24] A. Troutier, T. Delair, C. Pichot, C. Ladavière, Physicochemical and Interfacial Investigation of Lipid/Polymer Particle Assemblies, *Langmuir* 21 (2005) 1305-1313.
- [25] H. Wang, P. Zhao, W. Su, S. Wang, Z. Liao, R. Niu, J. Chang, PLGA/Polymeric Liposome for Targeted Drug and Gene Co-Delivery, *Biomaterials* 31 (2010) 8741-8748.
- [26] D.D. Lasic, Structure and Structure-Activity Relationships of Lipid-based Gene Delivery Systems, in: L. Huang, M.C. Hung, E. Wagner (Eds.), *Nonviral Vectors for Gene Therapy*, Academic Press, San Diego, 1999, pp. 69–89.
- [27] L. Ciani, S. Ristori, C. Bonechi, C. Rossi, G. Martini, Effect of the Preparation Procedure on the Structural Properties of Oligonucleotide/Cationic Liposome Complexes (Lipoplexes) Studied by Electron Spin Resonance and Zeta Potential, *Biophys. Chem.* 131 (2007) 80-87.

- [28] B.S. Aytar, J.P.E. Muleer, Y. Kondo, Y. Talmon, N.L. Abbott, D.M. Lynn, Redox-based Control of the Transformation and Activation of siRNA Complexes in Extracellular Environments Using Ferrocenyl Lipids, *J. Am. Chem. Soc.* 135 (2013) 9111-9120.
- [29] C.R. Safinya, Structures of Lipid-DNA Complexes: Supramolecular Assembly and Gene Delivery, *Curr. Opin. Struct. Biol.* 11(4) (2001) 440-488.
- [30] C. Leal, N.F. Bouxsein, K.K. Ewert, C.R. Safinya, Highly Efficient Gene Silencing Activity of siRNA Embedded in a Nanostructured Gyroid Cubic Lipid Matrix, *J. Am. Chem. Soc.* 132 (2010) 16841-16847.
- [31] J.O. Rädler, I. Koltover, T. Salditt, C.R. Safinya, Structure of DNA-Cationic Liposome Complexes: DNA Intercalation in Multilamellar Membranes in Distinct Interhelical Packing Regimes, *Science* 275 (1997) 810-814.
- [32] T. Kaasgaard, C.J. Drummond, Ordered 2-D and 3-D nanostructured amphiphile self-assembly materials stable in excess solvent, *Phys. Chem. Chem. Phys.* 8 (2006) 4957-4975.
- [33] R. Koynova, B. Tenchov, Cationic lipids: molecular structure/ transfection activity relationships and interactions with biomembranes, *Top. Curr. Chem.* 296 (2010) 51-93.
- [34] B. Tenchov, R. Koynova, Cubic phases in phosphatidylethanolamine dispersions: Formation, stability and phase transitions, *Chem. Phys. Lipids.* 208 (2017) 65-74.
- [35] E. Shyamsunder, S.M. Gruner, M.W. Tate, D.C Turner, P.T. So, C.P. Tilcock, Observation of inverted cubic phase in hydrated dioleoylphosphatidylethanolamine membranes, *Biochemistry* 27 (1988) 2332-2336.
- [36] J. Erbes, C. Czeslik, W. Hahn, R. Winter, M. Rappolt, G. Rapp, On the existence of bicontinuous cubic phases in dioleoylphosphatidylethanolamine, *Ber. Bunsenges. Phys. Chem.* 98 (1994) 1287-1293.
- [37] R. Koynova, L. Wang, R.C. Macdonald, Cationic phospholipids forming cubic phases: lipoplex structure and transfection efficiency, *Mol. Pharm.* 5 (2008) 739-744.
- [38] M. Muñoz-Ubeda, A. Rodríguez-Pulido, A. Nogales, A. Martín-Molina, E. Aicart, E. Junquera, Effect of lipid composition on the structure and theoretical phase diagrams of DC-Chol/DOPE-DNA lipoplexes, *Biomacromolecules* 11 (2010) 3332-3340.
- [39] M.P. Gantier, B.R.G. Williams, The response of mammalian cells to double stranded RNA, *Cytokine Growth Factor Rev.* 18 (2007) 363-371.
- [40] M. Olejniczak, P. Galka, W.J. Krzyzosiak, Sequence-non-specific effects of RNA interference triggers and microRNA regulators, *Nucleic Acid Res.* 38 (2010) 1-16.
- [41] G.N. Barber, Cytoplasmic DNA innate immune pathways, *Immunol. Rev.* 243 (2011) 99-108.

[42] A. Dady, E. Havis, V. Escriou, M. Catala, J.L. Duband, Junctional neurulation: a unique developmental program shaping a discrete region of the spinal cord highly susceptible to neural tube defects, *J. Neurosci.* 34 (2014) 13208-13221.